Viscoplastic Deformation of an Epoxy Resin at Elevated Temperatures

E. Kontou

Department of Applied Mathematical and Physical Sciences, Section of Mechanics, National Technical University of Athens, GR-15773, Athens, Greece

Received 25 October 2005; accepted 10 November 2005
DOI 10.1002/app.23768
Published online in Wiley InterScience (www.interscience.wiley.com).

ABSTRACT: The tensile behavior under monotonic loading and stress-relaxation testing of an epoxy resin has been studied. Experimental data at various strain rates and three temperatures from ambient up to just below T_g were performed, to study the transition from the brittle behavior to a ductile and therefore viscoplastic one. Dynamic mechanical analysis was applied to study the glass transition region of the material. Furthermore, a three-dimensional viscoplastic model was used to simulate the experimental results. This model incorporates all features of yield, strain softening, strain hardening, and rate/temperature dependence. The multiplicative decomposition of the deformation tensor into an elastic and viscoplastic part has also been applied, following the element arrangement in the mechanical model. A stress-dependent viscosity was controlling the stress–strain material behavior, involving model parameters, calculated from the Eyring plots. A new equation for the evolution of the activation volume with deformation was proposed, based on a probability density function. The model capability was further verified by applying the same set of parameters to predict with a good accuracy the stress-relaxation data as well. © 2006 Wiley Periodicals, Inc. J Appl Polym Sci 101: 2027–2033, 2006

Key words: viscoplasticity; Eyring model; activation volume evolution

INTRODUCTION

The mechanical behavior of amorphous glassy polymers at room temperature has been extensively studied, and the corresponding constitutive equations have been introduced in a wide strain rate range. In the glassy state, amorphous polymers exhibit either nonlinear viscoelastic–viscoplastic or brittle behavior. Ductile response is easily observed in glassy polymers at temperatures close to the glass transition T_g. Generally, at temperatures higher than T_g the behavior of polymers is described by the rubber elasticity theory or chain reptation. Constitutive models for the stress–strain behavior of polymers below, through and above T_g have been presented in earlier works.[1–3]

Below and near T_g a combination of rubbery behavior and that due to the intermolecular interaction is observed. Different physical approaches have been introduced to provide a description of mechanical behavior of glassy polymers at finite deformations.[4–8] The viscoelastic and viscoplastic deformations of amorphous polymeric materials has been related to their microstructural state.[4,9,10] Yield and plastic flow in glassy polystyrene has been extensively studied[11,12] in a wide range of molecular weights. Their constitutive response was examined in terms of a physically based three-dimensional constitutive model for small or large deformations in amorphous polymers.[13] The above model named "glass-rubber" constitutive model displays glassy response at low temperatures and short time scale, and rubber like response at high temperatures and long-time scales. Its main assumption is the additivity of free energies of bond distortion and conformation perturbation. Correspondingly, linear elasticity, Eyring viscous flow, and the Edwards–Vilgis entropy function have been employed, while the temperature dependence was introduced through Arrhenius equation. Later, Dooling et al.,[14] based on the glass–rubber constitutive model of Buckley and Jones,[13] developed a 3D constitutive model for large deformations, that captures the major features of response, which are observed experimentally on both sides of the T_g. It was demonstrated that this model appears wider applicability, as it has been applied for high molecular weight polymethylmethacrylate (PMMA). Moreover, this model was extended to include a relaxation spectrum for the conformational stresses appropriate to fit the high molecular weight PMMA. The three-dimensional finite deformation of amorphous polymers regarding the plastic flow process, strain softening, and the strain hardening response has been extensively described in a series of works.[15–17] Most of these works are based on the rate dependence of yield stress, or equivalently the defor-

Correspondence to: E. Kontou (ekontou@central.ntua.gr).

© 2006 Wiley Periodicals, Inc.

mation behavior is described by a single relaxation time, dependent on equivalent stress. Later in a work by Tervoort et al.[18] a "compressible-Leonov model " was introduced in which the elastic volume response is rigorously separated from the elasto-viscoplastic isochoric deformation. The deviatoric response was determined by a stress-dependent relaxation time, while the volume response remains elastic.

In the present work, the deformation behavior at small and finite strains of an epoxy glassy polymer has been studied. The material was chosen as a typical amorphous glassy polymer that includes chemical crosslinks. With varying temperature its behavior is transformed from a brittle to a ductile one. In this case, the material exhibits strong rate dependent effect. Tensile tests at three strain rates and at three temperatures, from ambient up to temperature close to the T_g, were performed. Also stress relaxation experiments were performed at a constant strain level with varying temperature. The material behavior was described using a viscoplastic model consisting of a nonlinear Maxwell model, that involves an Eyring dashpot, in parallel with a Langevin spring. With this model, the yield behavior of the polymeric material is described, using a stress-dependent relaxation time, while the Langevin spring accounts for the postyield strain hardening stage. The strain softening was formulated assuming an activation volume evolution in respect to deformation through a probability density function. The model was proved to be capable of capturing the main features of material response, with the same set of parameters for both tensile and stress-relaxation experiments.

MATERIALS AND METHODS

The material which was selected to be studied was an epoxy resin under the commercial name DERAKANE 411–45. It is based on a bisphenol-A glycidylether mixed with methacrylic acid. Benzoyl peroxide was used as an initiator. Curing takes place at room temperature, and a post curing procedure at 85°C for 5 h has been applied. The physical properties of the epoxy resin used are: viscosity = 440 cP, density = 1.04 g/cm^3, and gel time = 10–60 min. Dumbell specimens under the average dimensions 15 mm width, 3 mm thickness, and an average gauge length of 100 mm, were used for the tensile testing. The tensile experiments were performed at room temperature with an Instron 1121 type tester at three different strain rates, namely 8.33×10^{-5}, 3.33×10^{-4}, 1.66×10^{-3} sec^{-1}. The deformation could be measured very accurately at every localized region, along the total gauge length. The experimental procedure followed, is based on a noncontact method with a laser extensometer, described in detail in a previous work.[19] This method permits the noncontact measurement of the longitudinal deformation distribution along the specimen gauge length. For the axial elongation measurements a contrasting tape pattern code was applied, in terms of a number of white stripes on dark ground. True stress–strain curves were then constructed in respect to that part of the gauge length with the maximum strain. Correspondingly, tensile tests at the same strain rates were performed at temperatures 60 and 80°C with a high temperature chamber series 3119–406 of Instron Ltd.

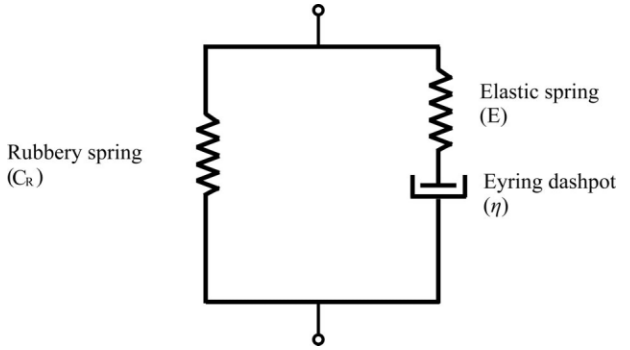

Figure 1 Schematic presentation of the mechanical model in one dimension.

Dynamic mechanical analysis (DMA) experiments were performed using the PerkinElmer DMA 7e instrument. The mode of deformation applied was three point bending, and the mean dimensions of samples were 4 mm × 20 mm, while the mean thickness was 3 mm. The temperature range varied from −100°C up to 220°C. The temperature dependent behavior was studied by monitoring changes in force and phase angle, keeping the amplitude of oscillation constant. The frequency was 1 Hz and the heating rate 5°C/min. The T_g value of the material, as obtained from the peak temperature of tan δ, was around 90°C.

Moreover, stress-relaxation experiments were carried out at 60 and 80°C, with the same Instron tester. The sample was subjected to an initial elongation, which corresponds to a strain equal to 0.015, with a crosshead speed of 200 mm/min. The Instron panel was modified to allow interfacing to a computer for full information of the test. The variation of load versus time was recorded with a sampling rate of 1.8 pt/s over a period of 2 h. Data recorded within the first 10 s after the initial application of strain were not used in calculations, to ensure that a true state of stress is being observed.

CONSTITUTIVE ANALYSIS

The mechanical model, shown in Figure 1, consists of a nonlinear Maxwell model connected in parallel with a Langevin spring. The Maxwell element involves a linear elastic spring which is related to the initial

elastic response, and an Eyring dashpot to account for the nonlinear viscoplastic material response. This element is capable of capturing the rate and temperature dependence, which is a main feature of polymeric structure. The Langevin spring has to do with the entropy change, because of the molecular alignment of macromolecular chains at high strains. The arrangement of these elements results in the expression:

$$\mathbf{F} = \mathbf{F}^e\mathbf{F}^v \tag{1}$$

where $\mathbf{F}$ is the total deformation gradient tensor, $\mathbf{F}^e$ is the deformation gradient acting on the elastic spring, and $\mathbf{F}^v$ is the deformation gradient acting on the viscoplastic element (Eyring dashpot).[20] This decomposition suggests that there is an intermediate configuration, obtained from the current configuration by unloading to a zero stress state. The total deformation gradient tensor $\mathbf{F}$ acts also on the Langevin spring, and therefore concerns the rubbery behavior of the material. The multiplicative decomposition of the deformation gradient in eq. (1), into the elastic and plastic part, introduced by Lee,[21] has been extended here to combine the elastic and viscoplastic parts. Analogous treatments have been applied in a series of works.[13,14,22]

Following eq. (1) the velocity gradient tensor of the viscoplastic contribution is given by:

$$\mathbf{L}^v = \dot{\mathbf{F}}^v\mathbf{F}^{v^{-1}} = \mathbf{D}^v + \mathbf{W}^v \tag{2}$$

where $\mathbf{D}^v$ and $\mathbf{W}^v$ are the symmetric and antisymmetric part of $\mathbf{L}^v$ and express the viscoplastic stretch rate and viscoplastic spin tensor correspondingly. It will be assumed that $\mathbf{W}^v = 0$, since our analysis includes tensile testing of an isotropic material, and the total spin $\mathbf{W}$ is also equal to zero.

Taking into account the non-Newtonian fluid relationship that must be valid for the Eyring dashpot of the mechanical model, and generalizing into a three dimensional problem, we have:

$$\mathbf{T}^v = 2\eta(\tau_{\text{eq}})\,\mathbf{D}^v \tag{3}$$

where $\mathbf{T}^v$ is the stress acting on the viscoplastic element and $\eta(\tau_{\text{eq}})$ is a stress-dependent (Eyring type) viscosity that will be analytically defined in the following. For a more accurate description, $\mathbf{T}^v$ should be replaced by $\mathbf{T}^{v^*} = \mathbf{R}^{v^T}\mathbf{T}^v\mathbf{R}^v$ where $\mathbf{T}^{v^*}$ is the stress transformed to its relaxed configuration.

Moreover, the total Cauchy stress will be given by:

$$\mathbf{T} = \mathbf{T}^v + \mathbf{T}^R \tag{4}$$

where $\mathbf{T}^R$ is the stress related with the Langevin spring (hyperelastic response).

When the yield flow procedure is modeled using an Eyring-flow process, it is assumed that the free energy barrier for molecular jumping becomes asymmetric with the application of stress.[23,24] For a one-dimensional process, the Eyring model gives:

$$\dot{\gamma}^p = \frac{1}{A}\sin\text{h}\left(\frac{\tau V_0}{RT}\right) \tag{5}$$

where $\dot{\gamma}^p$ is the plastic shear rate, τ is the applied shear stress, V_0 is the activation volume, R the gas constant, and T is the temperature. A is given by:

$$A = A_0\exp\left(-\frac{\Delta H}{RT}\right) \tag{6}$$

with A_0 the fundamental vibration frequency and ΔH the activation energy.

Setting $\tau_0 = RT/V_0$ eq. (5) can be rewritten as:

$$\tau = \tau_0\,\text{arc sin h}(A\dot{\gamma}^p) \tag{7}$$

Through eq. (7) a viscosity can be defined as:

$$\eta(\dot{\gamma}^p) = \frac{\tau}{\dot{\gamma}^p} = \frac{\tau_0\,\text{arc sin h}(A\dot{\gamma}^p)}{\dot{\gamma}^p} \tag{8}$$

Eyring model (eq. (5)) can be generalized into three dimensions as follows[18,24]:

$$\dot{\gamma}_{\text{eq}} = \frac{1}{A}\sin\text{h}\left(\frac{\tau_{\text{eq}}V_0}{RT}\right) \tag{9}$$

where

$$\tau_{\text{eq}} = \sqrt{\frac{1}{2}tr(\mathbf{T}^v\cdot\mathbf{T}^v)} \tag{10}$$

and

$$\dot{\gamma}_{\text{eq}} = \sqrt{2(\mathbf{D}^v\cdot\mathbf{D}^v)} \tag{11}$$

Approximating hyperbolic sine function we have:

$$\dot{\gamma}_{\text{eq}} = \frac{1}{A}\exp\left(\frac{\tau_{\text{eq}}}{\tau_0}\right) \tag{12}$$

Consequently, a generalized stress-dependent viscosity is obtained:

$$\eta(\dot{\gamma}_{\text{eq}}) = \frac{\tau_{\text{eq}}}{\dot{\gamma}_{\text{eq}}} = A\tau_0\left(\frac{\tau_{\text{eq}}}{\tau_0}\right)\exp\left(-\frac{\tau_{\text{eq}}}{\tau_0}\right) \tag{13}$$

Equation (13) expresses the stress dependence of Eyring viscosity. At low stress where $\tau_{\text{eq}} \ll \tau_0$ the

viscosity is equal to the zero-shear viscosity $\eta_0 = A\tau_0$. The main concept of Eyring equation is that deformation procedure at low stresses is accelerated by stress.[20]

Effects such as the pressure dependence of yielding as well as strain softening have been incorporated into the Eyring equation.[24,25]

As deformation proceeds, the molecular chains tend to align along the directions of principal plastic stretches. The configurational entropy of the system is then decreased and an internal network-stress state is created. This back stress, is the stress acting on the hyperelastic rubbery spring and can be modeled through a statistical mechanics of rubber elasticity model[15,17]:

$$\mathbf{T}^R = C_R \frac{\sqrt{N}}{3}\left[\lambda_i \mathrm{L}^{-1}\left(\frac{\lambda_i}{\sqrt{N}}\right) - \frac{1}{3}\sum_{j-1}^{3}\lambda_j \mathrm{L}^{-1}\left(\frac{\lambda_i}{\sqrt{N}}\right)\right] \quad (14)$$

where C_R is a rubbery modulus, N is the number of rigid chain links between chemical crosslinks, and λ_i are the principal stretch ratios, obtained by the total deformation gradient $\mathbf{F}$.L^{-1} is the inverse Langevin function.

This element can be related with a prominent feature of polymeric response: that is the strain hardening at large strains, which is considered to result from the Gaussian nature of the entropy function at large strains, due to the molecular alignment. This effect was observed experimentally by several techniques. Usually, constitutive modeling of strain hardening behavior is based on the concept of entanglements. In the well known Haward and Thackray[26] model, both the rubber-elastic response and finite extensibility were incorporated. Later, it was extended into a 3-D finite strain formulation.[15] Moreover, a neoHookean relation up to high draw ratios could describe strain hardening behavior in a Leonov model, consisting of a linear compressible spring and an Eyring dashpot.[18,27,28]

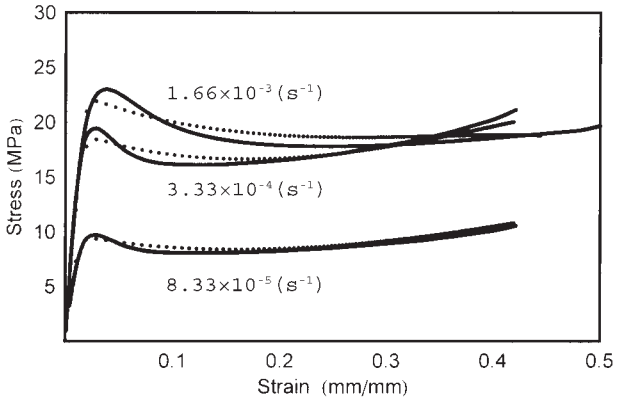

Figure 3 Tensile stress–strain curves of the epoxy resin at 60°C at three different strain rates. Thick lines: experimental data. Dotted lines: simulated results.

RESULTS AND DISCUSSION

Tensile testing

Uniaxial tensile tests at three different strain rates and three different temperatures were performed. The corresponding true stress–strain curves are presented in Figures 2–4. The epoxy polymer at room temperature shows a brittle behavior, exhibiting not a specific yield point, but rather a nonlinear behavior, while the rate dependence is negligible. At higher temperatures, namely 60 and 80°C the stress–strain response of the material changes significantly. The main features of mechanical behavior of a glassy polymer are exhibited: initially an elastic–viscoelastic response, afterwards nonlinear viscoelastic–viscoplastic, strain softening after yielding followed by a subsequent strain hardening. A strong rate dependence is also obtained. The transition from brittle to ductile response is attrib-

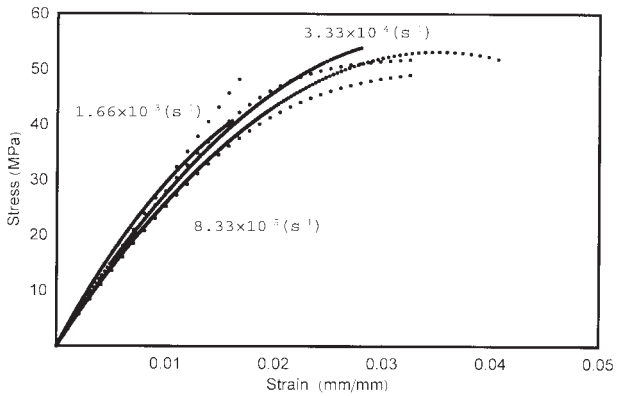

Figure 2 Tensile stress–strain curves of the epoxy resin at 20°C at three different strain rates. Thick lines: experimental data. Dotted lines: simulated results.

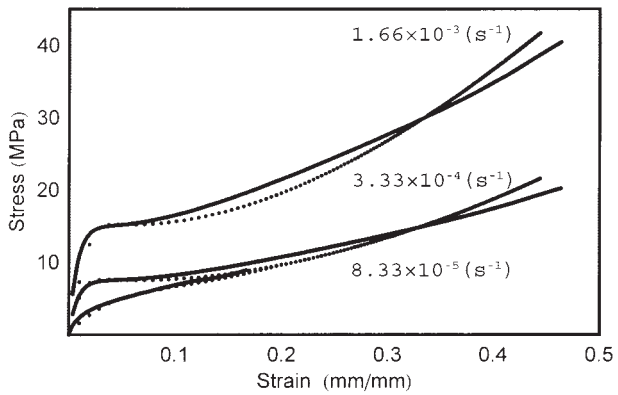

Figure 4 Tensile stress–strain curves of the epoxy resin at 80°C at three different strain rates. Thick lines: experimental data. Dotted lines: simulated results.

uted to the temperature effect. As it was obtained from DMA tests, the T_g of the material is around 90°C. Therefore, its behavior at 60°C and especially at 80°C which is a temperature close to the T_g is strongly affected by temperature.

From Figures 3 and 4 it is obvious that strain softening is more intense at 60°C, whereas strain hardening is substantially higher at 80°C. According to Wu and Buckley,[12] pronounced post yield softening in glassy polymers may be associated with initiation and propagation of highly localized shear bands.

It has been further shown[29] that in tests interrupted in the post yield region, and examined with a polarizing optical microscope, these shear bands were no more distinct. This is consistent with analogous observations in glassy polystyrene, where sharp shear bands at room temperature became more diffuse near the T_g.

Extending this observation in our tests, the strain softening that is manifested at 60°C for the epoxy resin examined, is negligible at 80°C, which is a temperature quite close to the T_g. The amount of strain softening is related to an evolution of structure, or equivalently to an evolution of free volume.[10] The free-volume theory considers the ease of local chain segment rotation during structural relaxation and inelastic deformation to depend on the amount of excess volume "frozen within the glassy state" available locally. In fact, the disordered nature of the glassy state means that the polymer will have a distribution of energy barriers for activated processes, such as stress induced shear transformation events.[10]

Calorimetric measurements during the deformation of several glassy polymers have revealed that the internal energy of the sample initially increases with strain, but levels off at about the steady state flow stress, suggesting that the material state stops evolving. Moreover, in a more nonequilibrated state, it will have higher initial free volume.[10]

Taking into account all this evidence, to formulate strain softening, the free volume will be treated as an internal state variable, which evolves with inelastic straining. In our analysis, free volume acquires a broader meaning, incorporating the concept of holes, the defects as well as the space necessary for the cooperative rearrangement of a group of molecular segments, i.e., the activation volume. Hence, it will be assumed that the "activation volume" associated with those regions follows a normal Gaussian distribution with a mean value m and a standard deviation s. Consequently, the strain evolved around those regions follows a similar distribution.[30]

Therefore, the distribution density in respect to strain ε_i as a random variable will be given by:

$$f(\tilde{\varepsilon}_i) = \frac{1}{s\sqrt{2\pi}} \exp\left[-\frac{1}{2}\left(\frac{\tilde{\varepsilon}_i - m}{s}\right)^2\right] \tag{15}$$

The fraction of activation volume that increased due to deformation will be given by the probability:

$$P = \frac{1}{s\sqrt{2\pi}} \int_0^{\varepsilon} e^{-\frac{1}{2}\left(\frac{\tilde{\varepsilon}_i - m}{s}\right)^2} d\tilde{\varepsilon}_i \tag{16}$$

where $\tilde{\varepsilon}_i$ is the equivalent strain.

At small strains the activation volume has an average initial value V_0, which at the yield point starts increasing up to a constant value, compatible with a saturated material state, which is attained with inelastic straining. This state of saturation is related with the emergence of steady state flow, where the material state stops evolving.

Let the activation volume at small strains to be equal to V_0. The increased fraction due to deformation will be equal to the probability P of eq. (16). Then at the subsequent stages of strain the new activation volume V for every stage of deformation will be given by:

$$V = V_0 + P\,V_0. \tag{17}$$

According to the Eyring theory, yielding initiates when the plastic strain rate becomes equal to the imposed effective strain rate, and following eq. (12), the activation volume V_0 at the onset of yielding can be calculated as follows: Writing eq. (12) in respect to a tensile test, $\tau_{eq} = \sigma_y/\sqrt{3}$, with σ_y the tensile yield stress, and $\dot{\gamma}_{eq} = \dot{\varepsilon}\sqrt{3}$, (where $\dot{\varepsilon}$ is the imposed strain rate) and solving for σ_y we obtain:

$$\sigma_y = \sqrt{3}\tau_0 \ln \dot{\varepsilon} + \sqrt{3}\,\tau_0 \ln(A\sqrt{3}) \tag{18}$$

From the above equation it follows that parameters τ_0 and A can be determined from the corresponding Eyring plots. For our experiments the Eyring plots are shown for both temperatures in Figure 5. The solid lines are the best fit of the parameters τ_0 and A. The parameter values calculated at the two temperatures are shown in Table I.

Numerical calculations were made using the software Mathematica[31] for step integration of the corresponding equations in the following way: starting from the deformation gradient tensor $\mathbf{F}^v$ at the initial unloaded condition, following eq. (2), a set of differential equations with unknown quantities the elements of $\dot{\mathbf{F}}^v$ is created. Combining eqs. (3), (10), and (13) and considering that $\mathbf{W}^v = 0$ the tensor $\mathbf{F}^v$ could be evaluated, as well as the tensor $\mathbf{D}^v$. Hereafter, through eq. (1) the elastic deformation gradient tensor $\mathbf{F}^e$ can be calculated, as well as the elastic and viscoplastic components of strain by the expressions:

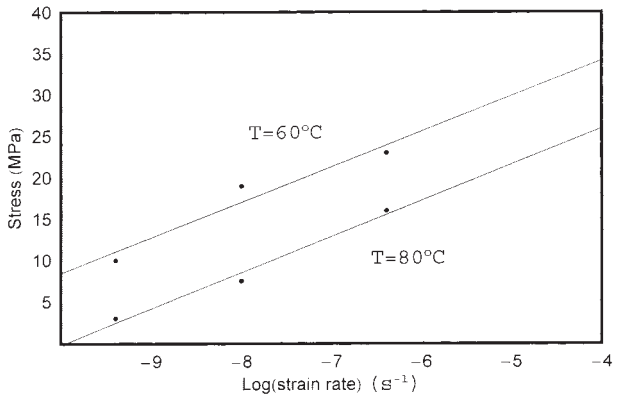

Figure 5 Eyring plots for tensile testing at two different temperatures.

$$\mathbf{E}^e = \frac{1}{2}(\mathbf{F}^{eT}\mathbf{F}^e - \mathbf{I}) \text{ and } \mathbf{E}^v = \frac{1}{2}(\mathbf{F}^{vT}\mathbf{F}^v - \mathbf{I}) \qquad (19)$$

where **I** is the identity matrix tensor.
In every step of calculation the stress dependent rate viscosity can be estimated, through the above-mentioned parameters η_0,τ_0. The equivalent stress τ_{eq} was calculated at every step of numerical calculation in terms of eq. (10).

The total stress tensor **T** versus total strain was then obtained combining eqs. (3),(4), and (14). The formulation of the strain softening that is mainly exhibited at 60°C has been made, taking into account the gradual increment of activation volume V_0 with increasing deformation, in terms of eq. (17). The mean value m was fitted to be 0.05 and the standard deviation s was equal to the one third of the mean value. The rubbery modulus C_R was estimated as 16 MPa at 60°C and 36 MPa at 80°C, and parameter N equal to 10. The simulated results at all strain rates and temperatures examined are plotted in Figures 2–4 in comparison with the experimental data. From these plots a satisfactory agreement is obtained for all cases.

Stress relaxation tests

Stress relaxation tests were performed at 60 and 80°C. At room temperature the epoxy material exhibits negligible time dependent behavior. The stress-relaxation curves are depicted in Figures 6(a) and 6(b). This behavior can be formulated with a stress-relaxation

TABLE I
Model Parameter Values

Temperature (°C)	τ_0 (MPa)	A (s)	V_0 (nm^3)	η_0 (MPa s)
60	2.473	91363	1.858	226022
80	2.516	12140	1.936	30545

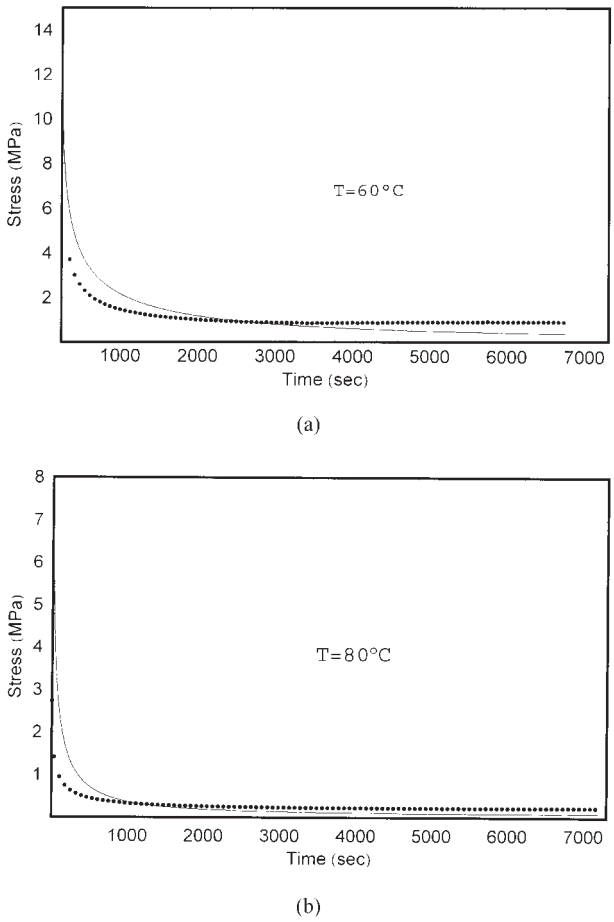

Figure 6 (a) Stress relaxation curve of the epoxy resin at 60°C and (b) Stress relaxation curve of the epoxy resin at 80°C.

function $Y(t)$, which can be written following the mechanical viscoplastic model of Figure 1 and considering a nonlinear Maxwell model. This nonlinearity is expressed in terms of the exponent b, as well as the stress-dependent relaxation time λ. Therefore we have:

$$Y(t) = C_{RN} + E\exp\left(-\frac{t}{\lambda}\right)^b \qquad (20)$$

where C_{RN} is a rubbery modulus related with the Langevin spring, E is the modulus of the material, which is affected by temperature, and λ is the stress-dependent relaxation time given by:

$$\lambda = \frac{\eta}{E} = \frac{\eta_0\frac{\tau_{eq}}{\tau_0}\exp\left(-\frac{\tau_{eq}}{\tau_0}\right)}{E} \qquad (21)$$

Exponent b further denotes the nonlinear material behavior, as well as the distribution of relaxation times, that is necessary to describe real material behavior.

The same parameter values for η_0, τ_0, as evaluated by tensile testing, were applied to simulate the stress-relaxation experiments. The quality of fitting is shown in Figures 6(a) and 6(b), and it is extracted that the applied viscoplastic model is capable of capturing the stress-relaxation behavior of the epoxy material studied. The rubbery modulus was fitted to be equal to 0.05 E, and exponent b equal to 0.3. The values of the elastic spring modulus E were scaled with temperature as follows: 3000, 1350, and 800 MPa at 20, 60, and 80°C correspondingly. These values were calculated from the initial slope of the corresponding stress–strain curves.

CONCLUSIONS

The tensile behavior under monotonic loading, as well as stress-relaxation testing has been examined for an epoxy resin. Experiments were performed at various temperatures and strain rates. The material behavior was simulated with the application of a 3D viscoplastic model, consisting of a nonlinear Maxwell in parallel with a Langevin spring. The total deformation gradient tensor related with the mechanical model was decomposed into an elastic and a viscoplastic part. The non-Newtonian constitutive equation for the Eyring dashpot expresses a flow rule that leads to the calculation of tensor $\mathbf{D}^v$. A stress dependent viscosity was then calculated, and was controlling the deformation material response. The activation volume was assumed to follow a normal Gaussian distribution, and then strain softening was formulated assuming an activation volume evolution in respect to deformation. A satisfactory agreement between experimental stress–strain data and stress-relaxation results and the simulated results was obtained using the same set of model parameters.

References

1. Gauthier, C.; Ladouce, D. L.; Quinson, L.; Perez, R. J. J Appl Polym Sci 1996, 65, 2517.
2. Boyce, M. C.; Socrate, S.; Llana, P. G. Polymer 2000, 41, 2183.
3. Chow, T. S. J Polym Sci 1987, 25, 137.
4. Mangion, M. B. M.; Cavailler, J. Y.; Perez, J. Philos Mag A 1992, 66, 773.
5. Argon, A. S. Philos Mag 1973, 28, 839.
6. Escaig, B. Plastic Deformation and Semi-Crystalline Materials; Escaig, B., G'sell, C., Eds.; Les Éditions de Physique: Les Ulis, Paris, 1985; p 187.
7. Hasan, O. A.; Boyce, M. C. Polym Eng Sci 1995, 35, 331.
8. Rendell, R. W.; Ngai, K. L.; Fong, G. R.; Yee, A.; Bankert, R. J. Polym Eng Sci 1987, 27, 2.
9. Perez, J. Physique et Mécanique des Polymères Amorphes; Lavoisier Tec & Doc: Paris, 1992.
10. Hasan, O. A.; Boyce, M. C.; Li, X. S.; Berko, S. J Polym Sci Part B: Polym Phys 1993, 31, 185.
11. Qi, H. J.; Boyce, M. C. Mech Mater 2005, 37, 817.
12. Wu, J. J.; Buckley, C. P. J Polym Sci 2004, 42, 2027.
13. Buckley, C. P.; Jones, D. C. Polymer 1995, 36, 3301.
14. Dooling, P. J.; Buckley, C. P.; Rostami, S.; Zahlan, N. Polymer 2002, 43, 2451.
15. Boyce, M. C.; Parks, D. M.; Argon, A. S. Mech Mater 1988, 7, 15.
16. Arruda, E. M. Ph.D. Thesis, Massachusetts Institute of Technology, 1992.
17. Wu, P. D.; van der Giessen, E. J. Mech Phys Solid 1993, 41, 427.
18. Tervoort, T. A.; Smit, R. J. M.; Brekelmans, W. A. M.; Govaert, L. E. Mech Time-Depend Mater 1998, 1, 269.
19. Spathis, G.; Kontou, E. Polymer 1998, 39, 135.
20. Eyring, H. J Chem Phys 1936, 4, 283.
21. Lee, E. H. ASME J Appl Mech 1969, 36, 1.
22. Krausz, A.; Eyring, H. Deformation Kinetics; Wiley-Interscience: New York, 1975.
23. Ward, I. M. Mechanical Properties of Solid Polymers, 2nd ed.; Wiley: Chichester, 1990.
24. Tervoort, T. A.; Klompen, E. T. J.; Govaert, L. E. J Rheol 1996, 40, 779.
25. Kontou, E.; Spathis, G. Polym Eng Sci 1998, 38, 1443.
26. Haward, R. N.; Thackray, G. Proc R Soc London Ser A 1968, 302, 453.
27. Leonov, A. I. Rheol Acta 1976, 15, 85.
28. van Melick, H. G. H.; Govaert, L. E.; Meijer, H. E. H. Polymer 2003, 44, 3579.
29. Quinson, R.; Perez, J.; Rink, M.; Pavan, A. J Mater Sci 1997, 32, 1371.
30. Spathis, G.; Kontou, E. J Appl Polym Sci 2001, 41, 1337.
31. Wolfram, S. The Mathematica Book, 4th ed.; Wolfram Media/Cambridge University Press: Cambridge, UK, 1999.